

# Morphological and Tissue Characterization of Culprit Lesions in Patients with ST-Segment Elevation Myocardial Infarction After Thrombolytic Therapy. Analysis with Grayscale Intravascular Ultrasound and iMAP™ Technology

Cristiano Freitas de Souza<sup>1</sup>, Akiko Maehara<sup>1</sup>, Eduardo Lima<sup>2</sup>, Leonardo de Freitas C. Guimarães<sup>2</sup>, Antonio Carlos Carvalho<sup>2</sup>, Claudia M.R. Alves<sup>2</sup>, Adriano Caixeta<sup>3</sup>

## ABSTRACT

**Background:** Currently, there is a great debate about the pathophysiology of acute myocardial infarction and tissue composition and morphology of lesions responsible for ischemic events. However, few studies have investigated the applicability of tissue characterization using iMAP™ technology in these patients. We evaluated patients with ST-segment elevation myocardial infarction after thrombolytic therapy with grayscale intravascular ultrasound and iMAP™ technology to describe the tissue composition of the culprit lesions. **Methods:** Twenty-five ST-segment elevation myocardial infarction patients with successful reperfusion had the three major epicardial coronary arteries evaluated by grayscale intravascular ultrasound and iMAP™ technology. **Results:** Mean age was  $51 \pm 11.5$  years with a prevalence of males (72%). The artery most often involved was the right coronary artery (48%). Intravascular ultrasound showed that the culprit lesions were long (mean extension  $31.0 \pm 17.2$  mm) with a high percent of plaque volume ( $58.5 \pm 5.1\%$ ). At the point of highest obstruction (minimal luminal area), the plaque burden was  $82.5 \pm 7.5\%$ . Furthermore, the mean remodeling index was  $1.4 \pm 1.0$ , indicating positive remodeling. iMAP™ analysis of the lesion and minimal luminal area showed a prevalence of fibrotic and necrotic components when compared to other components. **Conclusions:** In ST-segment elevation myocardial infarction patients, the culprit lesion showed a prevalence of positive arterial remodeling and the necrotic core component in the composition of the culprit plaque corroborating *in vivo* the main pathophysiology of acute atherosclerotic disease.

**DESCRIPTORS:** Myocardial infarction. Plaque, atherosclerotic. Thrombolytic therapy. Ultrasonography.

## RESUMO

### Caracterização Morfológica e Tecidual de Lesões Culpadas em Pacientes com Infarto Agudo do Miocárdio com Supradesnivelamento do Segmento ST Após Uso de Fibrinolítico. Análise com Ultrassom Intracoronário e Tecnologia iMAP®

**Introdução:** Atualmente, existe grande debate acerca da fisiopatologia do infarto agudo do miocárdio e da composição tecidual e morfológica das lesões responsáveis por eventos isquêmicos. Entretanto, poucos estudos investigaram a aplicabilidade da tecnologia iMAP® na caracterização tecidual desses pacientes. Avaliamos pacientes com infarto agudo do miocárdio com supradesnivelamento do segmento ST pós-fibrinolítico com ultrassom intravascular em escala de cinzas e com a tecnologia iMAP®, a fim de descrever a composição tecidual das lesões culpadas pelo infarto agudo do miocárdio. **Métodos:** Foram avaliadas três artérias coronárias epicárdicas com ultrassom intravascular em escala de cinzas e com a tecnologia iMAP® de 25 pacientes com infarto agudo do miocárdio com supradesnivelamento do segmento ST pós-trombólise, com critérios de reperusão. **Resultados:** A média de idade foi de  $51 \pm 11,5$  anos, com predomínio do sexo masculino (72%). A artéria mais frequentemente envolvida foi a coronária direita (48%). O ultrassom intravascular mostrou que as lesões culpadas eram longas (extensão de  $31,0 \pm 17,2$  mm) e com elevado percentual de volume de placa ( $58,5 \pm 5,1\%$ ). No ponto de maior obstrução, ou seja, na área luminal mínima, a carga de placa foi de  $82,5 \pm 7,5\%$ . Além disso, o índice de remodelamento médio foi de  $1,4 \pm 1,0$ , denotando remodelamento positivo. As análises pelo iMAP®, tanto da lesão, quanto da área luminal mínima, mostraram predomínio em termos percentuais de componentes fibrótico e necrótico, quando comparados aos demais. **Conclusões:** As lesões ateroscleróticas culpadas pelo infarto agudo do miocárdio com supradesnivelamento do segmento ST apresentaram predomínio de remodelamento arterial positivo e do componente necrótico na composição da placa culpada, o que corrobora, *in vivo*, a principal fisiopatologia da doença aterosclerótica aguda.

**DESCRIPTORES:** Infarto do miocárdio. Placa aterosclerótica. Terapia trombolítica. Ultrassonografia.

<sup>1</sup> Cardiovascular Research Foundation, Columbia University Medical Center, New York, USA.

<sup>2</sup> Universidade Federal de São Paulo, São Paulo, SP, Brazil.

<sup>3</sup> Hospital Israelita Albert Einstein, São Paulo, SP, Brazil.

**Correspondence to:** Adriano Caixeta. Avenida Albert Einstein, 627/701 – Morumbi – CEP: 05652-900 – São Paulo, SP, Brazil  
E-mail: adriano.caixeta@einstein.br

Received on: 06/03/2014 • Accepted on: 08/18/2014

**A**cute myocardial infarction (AMI) is a clinical entity normally resulting from partial (non-ST-segment elevation MI – NSTEMI) or total thrombotic obstruction (ST-segment elevation MI – STEMI) of a epicardial coronary artery.<sup>1</sup> Pathological studies have shown that the triggering event in thrombus formation and subsequent vessel occlusion results from the rupture of a atherosclerotic fibrous cap in 60% of cases, from plaque erosion in 30 to 35%, and from a thrombus formation superimposed on calcium nodules in 5 to 10%.<sup>2,3</sup>

However, much is still debated about the composition of atherosclerotic plaques that develop from a condition considered stable to a situation of instability, with consequent outbreak of thrombotic events and acute coronary ischemia. In this situation, the intravascular ultrasound (IVUS) is an important tool in the identification and characterization of the morphology of atherosclerotic plaques related to AMI, although it is not possible to identify plaque erosion due to limitations in spatial resolution, a problem that can be overcome using optical coherence tomography (OCT).<sup>4,5</sup> The IVUS identifies plaque and calcium nodule rupture with high sensitivity and specificity. Additionally, several findings at IVUS are characteristic of unstable plaques, such as extensive positive remodeling<sup>6</sup> and the presence of small amounts of calcium with localized and scattered distribution (spotty calcification).<sup>7,8</sup> Recently, the application of tissue characterization with the iMAP™ technology (Boston Scientific, Santa Clara, United States) made further progress in the identification of atherosclerotic plaque composition, identifying and quantifying the lipidic and necrotic contents, which are directly related to lesion instability.<sup>9</sup> Unlike the VH-IVUS® technology (Volcano Corporation, San Diego, United States), there have been few clinical studies assessing the accuracy of iMAP™ in the characterization of atherosclerotic plaques involved in STEMI. Even scarcer are the studies of patients submitted to thrombolytic therapy, in whom IVUS can be performed in vessels without any type of previous intervention (pre-dilation and/or thrombus aspiration).

The present study aimed to describe the quantitative, morphological tissue findings and using IVUS with greyscale analysis and iMAP™ technology of culprit lesions in STEMI patients treated with fibrinolytic therapy.

## METHODS

### Patients and study design

From September 2011 to May 2012, 25 patients with clinical and electrocardiographic diagnosis of STEMI treated with fibrinolytic therapy were prospectively included in the study iWonder (Imaging WhOle vessel coroNary tree with intravascular ultrasounD and iMap in patiEnts with acute myocaRdial infarction). This study

included 100 patients with NSTEMI or STEMI, whether or not treated with fibrinolytic therapy, and analyzed, through IVUS, three epicardial coronary arteries, in greyscale and iMAP™, regarding the phenotypic and tissue characteristics of culprit and non-culprit lesions.<sup>10</sup> The project was conducted in the Hemodynamics and Interventional Cardiology Division of the Hospital São Paulo, Escola Paulista de Medicina, Universidade Federal de São Paulo, São Paulo, Brazil, having been previously approved by the Research Ethics Committee of the institution (project 0889/11, August 5, 2011) and registered in ClinicalTrials.org under number NCT01437553. All patients or their legal guardians were informed about the objectives and risks of study-related procedures, and signed an informed consent form prior to the diagnostic procedure.

As part of the present subanalysis, the inclusion criteria were age < 75 years; clinical-electrocardiographic diagnosis of STEMI with prior fibrinolytic therapy, with time of evolution < 30 days; identification, through coronary angiography, of the culprit lesion responsible for the clinical picture; and IVUS assessment availability. Exclusion criteria were: STEMI and target-vessel with Thrombolysis in Myocardial Infarction (TIMI) coronary flow equal to 0; previous percutaneous coronary intervention (PCI) or coronary artery bypass graft surgery (CABG); hemodynamic instability; Killip class III/IV; severe renal dysfunction (serum creatinine > 2.0 mg/dL and/or creatinine clearance ≤ 30 mL/minute); coronary anatomy unsuitable for IVUS performance; critical coronary obstruction preventing the passage of the IVUS catheter; total occlusion of any of three epicardial coronary arteries; stenosis > 50% in the left main coronary artery with indication for surgical revascularization; patient and/or legal guardian unable to or unwilling to sign the informed consent. Collection of peripheral blood samples for complete blood count, urea, creatinine, glucose, total cholesterol and fractions, ultrasensitive C-reactive protein (us-CRP), and glycated hemoglobin (HbA<sub>1c</sub>) was performed.

### Intravascular ultrasound procedure

The IVUS of epicardial coronary arteries was performed immediately after the diagnostic procedure, under patient's full heparinization (100 U/kg of unfractionated heparin, aiming at activated clotting time [ACT] between 250 and 350 seconds) and administration of an intracoronary vasodilator (100-200 µm of nitroglycerin). Initially, an IVUS study was performed in the artery related to the clinical event (culprit vessel), followed by angioplasty, when necessary. Subsequently, the other two coronary arteries unrelated to the clinical event (non-culprit vessels) were analyzed with IVUS. A 40-MHz IVUS catheter (Atlantis® SR Pro; Boston Scientific, Santa Clara, United States), was used with the

gray scale analysis and morphological characterization by using the iMAP-IVUS® modality (Boston Scientific, Santa Clara, United States). Automatic pullback movements of the ultrasound catheter were performed at a speed of 0.5 mm/s, starting at a 10-mm distal point from the culprit lesion, toward the arterial ostium. For non-culprit arteries, the same routine was performed for analysis of plaques unrelated to the event.

### Intravascular ultrasound image analysis

All angiography and IVUS images were stored in digital media and copied to an external hard drive for offline analysis at the Intravascular Image Laboratory of the Cardiovascular Research Foundation (New York, United States).

The IVUS analysis was performed in three sequential steps:

**1. Quantitative analysis:** quantitative volumetric analysis was performed according to current guidelines.<sup>11,12</sup> This phase of the offline IVUS analysis consisted in the definition of the segment to be analyzed in each pullback, including at least 10 mm of extension, distal to the respective vessel ostium. Subsequently, using the Qivus 2.1® software (Medis Medical Imaging Systems, Leiden, the Netherlands) the automatic contours of the vessel and lumen were obtained at every 1 mm within the defined segment. Then, using Simpson's method, the volumes of the lumen, vessel, and plaque (vessel minus lumen) were computed. The plaque burden was calculated as the ratio of the cross-sectional area of the plaque by the cross-sectional area of the vessel, multiplied by 100. The minimal luminal area (MLA) was defined as the smallest cross-sectional area of the lumen within the lesion. The stenosis area was calculated as the cross-sectional area of the lumen at the MLA divided by the cross-sectional area of the vessel in the reference segment, multiplied by 100. The cross-sectional area of the vessel in the reference segment was defined as the mean proximal and distal cross-sectional area of the vessel, at the point where the vessel had an aspect closest to normal, with the largest lumen and lowest plaque burden. When one of the two reference segments (proximal or distal) could not be measured, the calculation was based on only one of them. If none of the two segments could be measured, variables depending on reference measures were not calculated. The remodeling index was calculated as the cross-sectional area of the vessel at the MLA point divided by the cross sectional area of reference.

**2. Qualitative analysis:** plaque rupture was defined as an intraplaque cavity in communication with the lumen, in the presence of the fibrous-cap residues or fragments.<sup>13</sup> The plaque was considered as hypoechoic when it was predominantly (> 75%) less bright when

compared with the adventitia, and it was considered as hyperechoic when it was brighter (> 75%) than the adventitia. Calcium nodules were defined as a dense, eruptive, irregular surface mass, incontact with and/or near the lumen.<sup>14</sup>

**3. Tissue characterization by iMAP:** iMAP-IVUS® is a type of image that uses radio-frequency spectral analysis to obtain an algorithm to classify the atherosclerotic plaque into four components: fibrotic, lipidic, necrotic, and calcified. The development of this algorithm was based on *ex vivo*<sup>15</sup> histological analyses, and each component was assigned a color: green for the fibrotic component, yellow for the lipidic component, red for the necrotic component, and white for the calcified component (Figure 1).

Categorical variables were expressed as absolute and percentage frequencies, and continuous variables were expressed as means ± standard deviations.

### RESULTS

The mean age of patients was 51 ± 11.5 years, with a predominance of male patients (72%). The time between the index event and performance of the IVUS procedure was 7.2 ± 2.1 days. Among the risk factors for coronary artery disease (CAD), a high prevalence of diabetes (40%), hypertension (60%), and smoking (64%) was observed. Moreover, at admission, there were a low proportion of patients using acetylsalicylic acid (ASA), as none had had a previous ischemic event. The other clinical and angiographic characteristics are summarized in Table 1.

In the analysis of the culprit lesion by IVUS with gray scale (Table 2), long lesions (extension of 31.0 ± 17.2 mm) with high plaque volume (58.5 ± 5.1%) were

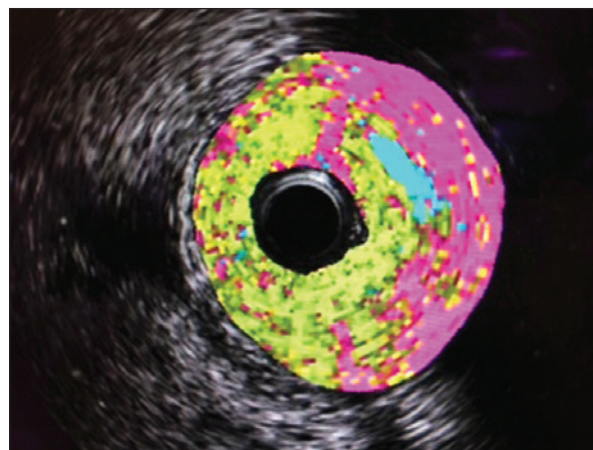


**Figure 1** – Intravascular ultrasound cross-sectional image with iMAP™ technology, depicting a large amount of necrotic (red) and fibrotic (green) component in addition to the lipid core (blue).

**TABLE 1**  
 Baseline clinical characteristics, laboratory tests, and drug therapy.

| Variables                          | n = 25       |
|------------------------------------|--------------|
| Age, years                         | 51.0 ± 11.5  |
| Male gender, n (%)                 | 18 (72)      |
| Body mass index, kg/m <sup>2</sup> | 26.5 ± 5.7   |
| Diabetes mellitus, n (%)           | 10 (40)      |
| Hypertension, n (%)                | 15 (60)      |
| Smoking, n (%)                     | 16 (64)      |
| Dyslipidemia, n (%)                | 9 (36)       |
| Laboratory tests on admission      |              |
| Total cholesterol, mg/dL           | 164.0 ± 70.5 |
| HDL cholesterol, mg/dL             | 35.0 ± 17.3  |
| LDL cholesterol, mg/dL             | 113.0 ± 42.6 |
| Triglycerides, mg/dL               | 109.0 ± 59.1 |
| Creatinine clearance, mL/min       | 92.0 ± 45.2  |
| us-CRP, mg/L                       | 5.5 ± 7.0    |
| Fasting glucose, mg/dL             | 116.0 ± 62.1 |
| Glycated hemoglobin, %             | 6.2 ± 2.7    |
| Culprit artery n (%)               |              |
| Left anterior descending artery    | 10 (40)      |
| Left circumflex artery             | 3 (12)       |
| Right coronary artery              | 12 (48)      |
| Medications at admission, n (%)    |              |
| ASA                                | 4 (16)       |
| Thienopyridines                    | 0            |
| ACEI/ARB                           | 13 (52)      |
| Statins                            | 6 (24)       |
| Beta-blockers                      | 8 (32)       |
| Medications at discharge, n (%)    |              |
| ASA                                | 25 (100)     |
| Thienopyridines                    | 25 (100)     |
| ACEI/ARB                           | 20 (80)      |
| Statins                            | 25 (100)     |
| Betablockers                       | 9 (36)       |

HDL: high-density lipoprotein; LDL: low-density lipoprotein; us-CRP: ultrasensitive C-reactive protein; ACEI: angiotensin-converting enzyme inhibitor; ARB: angiotensin II receptor blockers.

**TABLE 2**  
 Data from intravascular ultrasound in gray scale and of tissue composition with iMAP™.

| Analysis through grayscale of culprit lesion               | n = 25        |
|--|---------------|
| Vessel area in the distal reference MLA, mm <sup>2</sup>   | 8.9 ± 3.3     |
| Lumen area in the distal reference MLA, mm <sup>2</sup>    | 6.0 ± 2.1     |
| Plaque area in the distal reference MLA, mm <sup>2</sup>   | 3.2 ± 1.4     |
| Vessel area in the proximal reference MLA, mm <sup>2</sup> | 14.8 ± 4.6    |
| Lumen area in the proximal reference MLA, mm <sup>2</sup>  | 9.6 ± 2.7     |
| Plaque area in the proximal reference MLA, mm <sup>2</sup> | 5.4 ± 2.1     |
| Lesion extension, mm                                       | 31.0 ± 17.2   |
| Vessel volume, mm <sup>3</sup>                             | 427.4 ± 302.8 |
| Lumen volume, mm <sup>3</sup>                              | 175.3 ± 123.9 |
| Plaque volume, mm <sup>3</sup>                             | 257.7 ± 184.5 |
| Percentage of plaque volume, %                             | 58.5 ± 5.1    |
| Mean vessel area, mm <sup>3</sup> /mm                      | 14.3 ± 2.9    |
| Mean lumen area, mm <sup>3</sup> /mm                       | 5.6 ± 1.3     |
| Mean plaque area, mm <sup>3</sup> /mm                      | 8.9 ± 1.9     |
| <b>Gray scale analysis of lesion MLA</b>                   |               |
| Vessel area in MLA, mm <sup>2</sup>                        | 12.9 ± 3.2    |
| Lumen area in MLA, mm <sup>2</sup>                         | 2.0 ± 1.0     |
| Plaque area in MLA, mm <sup>2</sup>                        | 10.5 ± 3.1    |
| Plaque burden, %   | 82.5 ± 7.5    |
| Remodeling index   | 1.4 ± 1.0     |
| <b>Tissue analysis of the lesion through iMAP™</b>         |               |
| Necrotic component volume, mm <sup>3</sup>                 | 60.0 ± 65.6   |
| Calcified-component volume, mm <sup>3</sup>                | 6.1 ± 8.3     |
| Lipidic-component volume, mm <sup>3</sup>                  | 17.7 ± 16.2   |
| Fibrotic-component volume, mm <sup>3</sup>                 | 152.4 ± 112.8 |
| Necrotic-component/calcified-component ratio               | 10.6 ± 13.9   |
| Percentage of the necrotic-component volume, %             | 23.4 ± 9.2    |
| Percentage of the calcified-component volume, %            | 2.2 ± 1.8     |
| Percentage of the lipidic-component volume, %              | 7.1 ± 1.9     |
| Percentage of the fibrotic-component volume, %             | 65.6 ± 10.4   |
| <b>Tissue analysis in the MLA through iMAP™</b>            |               |
| Percentage of the necrotic-component volume, %             | 23.6 ± 14.8   |
| Percentage of the calcified-component volume, %            | 1.6 ± 1.7     |
| Percentage of the lipidic-component volume, %              | 6.4 ± 2.6     |
| Percentage of the fibrotic-component volume, %             | 63.4 ± 18.1   |

MLA: minimal luminal area.

observed. At the point of maximum obstruction (MLA), the lumen was 2.0 ± 1.0 mm<sup>2</sup>, while the measured plaque burden was 82.5 ± 7.5%. Consistent with the profile of patients studied, the mean rate of remodeling was > 1.05 (1.3 ± 1.0).

The lesion tissue analysis by iMAP™ showed a predominance, in percentage terms, of fibrotic and necrotic components, when compared to the others,

demonstrating greater vulnerability and instability of these lesions. This finding was similar to that observed at the point of maximum obstruction (MLA), also with a predominance of fibrotic and necrotic components.

Finally, the IVUS morphological analysis showed that the triggering event for thrombosis was coronary plaque rupture in 36% of cases (9/25), while calcium nodules were observed in only 4% of patients (1/25).

## DISCUSSION

The present study evaluated 25 patients with STEMI undergoing fibrinolytic therapy referred for coronary angiography and submitted to IVUS of all three epicardial coronary arteries. The main findings were: (1) culprit lesions showed findings consistent with a vulnerable plaque, such as large necrotic core (> 20%) and reduced calcified content; (2) plaque rupture was the underlying event for coronary thrombosis in 36% of cases; and (3) positive arterial remodeling was present in almost all the lesions. The present study provides, for the first time in literature, the description of the morphological characteristics of the plaque responsible for STEMI in patients after the use of fibrinolytic therapy using the iMAP™ tissue characterization technology. A potential advantage of this analysis when compared to previous studies lies in the fact that the IVUS analysis was performed after successful fibrinolytic therapy, minimizing the risk of thrombus interference in image interpretation.

Recent pathological studies have described the evolution stages of the atherosclerotic plaque, from the stable, incipient, and benign state, to more advanced stages of instability, leading to acute coronary events.<sup>2,16</sup> In the early stages of intimal thickening and intimal xanthoma, the atherosclerotic plaque is constituted mainly of focal accumulation of smooth muscle cells with extracellular matrix rich in proteoglycans, without signs of inflammation. From this stage onwards, atherosclerosis progression occurs with marked inflammatory component, represented mainly by macrophage infiltrates in the lipid core, and a decrease in proteoglycan and collagen in the fibrous cap. In the last phase of the natural course of atherosclerosis, this evolution process results in the formation of the so-called vulnerable plaque, represented by thin-cap fibroatheroma (TCFA), whose diagnostic findings are a large necrotic core (usually  $\geq 25\%$  of plaque area)<sup>17</sup> surrounded by a thin fibrous cap ( $\leq 65 \mu\text{m}$ ) and richly infiltrated by macrophages with reduced amount of smooth muscle cells.<sup>16,18</sup>

One of the most often studied findings associated with plaque vulnerability is arterial remodeling. Initially described by Glagov et al.<sup>19</sup> in 1987, the positive arterial remodeling has been observed in atherosclerotic plaques responsible for acute coronary events,<sup>6,20,21</sup> and is associated with the increase in CK-MB after PCI,<sup>22</sup> no-reflow phenomena during primary PCI,<sup>23</sup> recurrent ischemia after PCI,<sup>24</sup> major cardiovascular events in patients with unstable angina undergoing any form of revascularization,<sup>25</sup> and intimal hyperplasia after PCI with bare-metal<sup>26</sup> and drug-eluting stents.<sup>27</sup> In the present study, the mean arterial-remodeling index was  $1.4 \pm 1.0$ , greater than 1.05, thus characterizing the predominance of positive arterial remodeling and corroborating the aforementioned literature.

In addition to arterial remodeling, other data from the quantitative analysis of the IVUS in grayscale are

noteworthy. One is the quantification of the plaque burden, of the atheroma that has been previously shown to be directly associated with distal embolization.<sup>28</sup> Furthermore, in the VH-IVUS in Vulnerable Atherosclerosis (VIVA) study,<sup>29</sup> in which 170 patients with stable angina or acute coronary syndrome with troponin elevation were evaluated through IVUS of three vessels, one of the predictors of major adverse cardiovascular event during a mean follow-up of 625 days was the presence of plaque burden > 70%. Similarly, in the PROSPECT study,<sup>30</sup> which assessed 697 patients with acute coronary syndrome submitted to IVUS of the three arteries, one of the most significant predictors of major cardiovascular adverse event associated with non-culprit lesions during 3 years of follow-up was plaque burden > 70% (the other variables were the presence of TCFA and  $\text{MLA} \leq 4.0 \text{ mm}^2$ ). In the present analysis, involving only patients with STEMI, the plaque burden found in the culprit lesion was  $82.5 \pm 7.5\%$ . A recent subanalysis of the PROSPECT study<sup>31</sup> demonstrated that diabetic patients had even more significant findings related to plaque burden when compared to those without diabetes (56.8 vs. 55.0%;  $p = 0.0006$ ). In the present study, in an exploratory comparison, a similar numerical trend was observed, with the diabetic population showing higher plaque burden ( $84.4 \pm 9.0\%$ ) when compared to non-diabetic patients ( $81.5 \pm 6.4\%$ ), but without reaching statistical significance ( $p = 0.77$ ).

In relation to the event triggering the thrombosis and subsequent coronary-artery occlusion, it is well established in the literature that plaque rupture is responsible for most cases (60%).<sup>3,16</sup> In a recent study using OCT and comparing 80 patients with asymptomatic CAD and NSTEMI, Shimamura et al. demonstrated that symptomatic plaque rupture, i.e., associated with acute ischemic events, showed a higher number of plaques rich in lipids and thrombus, as well as lower MLA of the lesion and MLA at the peak of rupture.<sup>32</sup> Of the 25 culprit lesions analyzed in this study, plaque rupture was identified in 9 (36%) (Figure 2). This percentage, lower than that usually described, may have been a result of the long period of time between the index event and the performance of IVUS in some cases (mean time between index event and IVUS procedure:  $7.2 \pm 2.1$  days). Thus, it is possible that some ruptured plaques scarred, or that the cavity was filled by a thrombus, thus hindering their identification through IVUS. Recently, calcium nodules, also identifiable by IVUS, were associated with acute coronary syndrome in 5 to 10% of cases.<sup>33</sup> The mechanism by which calcium nodules result in coronary thrombosis is still unknown. In the present cohort, only one patient (4%) had a calcium nodule identified by IVUS (Figure 3), similar to the prevalence reported in previous studies.

When using tissue characterization through iMAP™, the characteristic finding of unstable plaques consists in the large amount of necrotic core. In a study by Missel

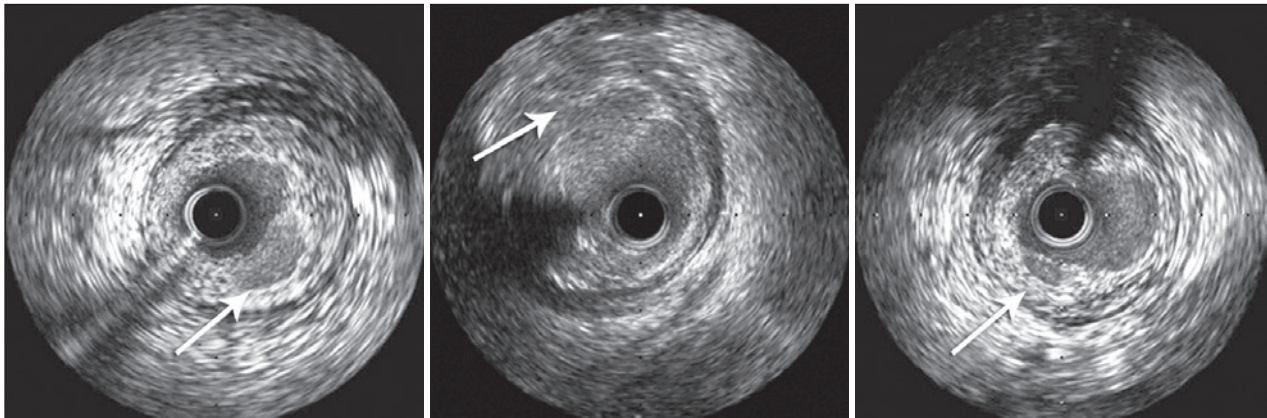


**Figure 2** – Intravascular ultrasound cross-sectional images in three different patients, showing examples of ruptured plaque (arrow) as the event that triggered the coronary thrombosis.

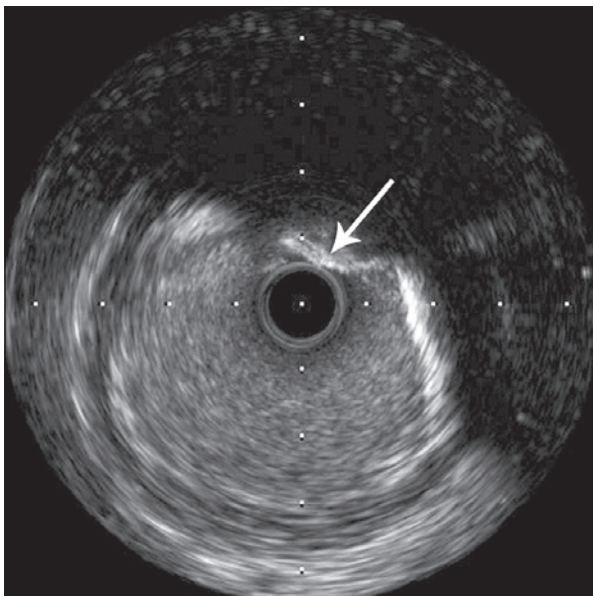


**Figure 3** – Intravascular ultrasound of the right coronary artery showing compatibility with calcium nodule (dense, eruptive mass, with irregular surface, in contact with and/or near the lumen, as indicated by the arrow).

et al.<sup>34</sup> using virtual histology, a correlation was found between a large necrotic core and reduced calcified component, with increased CK-MB release in patients with acute coronary syndrome. In this study, the volume of the necrotic core was found to be  $19.2 \pm 18.0 \text{ mm}^3$ , while the calcified component volume was  $1.4 \pm 13.9 \text{ mm}^3$ . Moreover, the authors demonstrated that higher-risk patients (those with CK-MB release and ST segment depression on ECG) presented high necrotic core/dense calcium ratio (NC/DC = 1.83, interquartile

range, 1.27 to 2.76) as a risk predictor. In the present study, which differed from the above mentioned study by evaluating patients at higher risk (STEMI) and with different tissue characterization technology, a necrotic core volume of  $60.0 \pm 65.6 \text{ mm}^3$  and calcified component of  $6.12 \pm 8.34 \text{ mm}^3$  were observed, and the NC/DC ratio was  $10.6 \pm 13.9$ . This demonstrates that there may be a correlation between a profile of more severe patients, represented by STEMI, and a larger number of necrotic components in culprit lesions.

In a contemporary study<sup>35</sup> comparing patients with AMI with or without ST-segment elevation, the mean percentage of necrotic component was found to be 37% in the STEMI group, while the calcified component was only 3%. In the present study, the mean percentage of the necrotic component was  $23.4 \pm 9.2\%$ , and the calcified component was  $2.17 \pm 1.76\%$ . These findings are similar when the full extent of the lesion or only the MLA are analyzed. In the present analysis, at the point of MLA, the mean percentage of necrotic component was  $23.6 \pm 14.8\%$  and the calcified component was  $1.62 \pm 1.70\%$ .

Finally, the results demonstrated using iMAP™ in patients with STEMI were similar to those previously published with VH-IVUS®, demonstrating its potential applicability in clinical practice.<sup>6-8</sup>

### Limitations

The present study has several limitations; the main ones are related to the low spatial resolution of IVUS, especially when compared to OCT. This can result in difficulty in the identification and quantification of the thrombotic component, which may be mistakenly classified as fibrotic component by iMAP™. However, unlike the OCT, the IVUS has greater wave penetration, allowing for the quantification of arterial remodeling,

for instance. Additionally, the guidewire artifact, while interfering minimally in image generation, may have been included in this analysis as necrotic component, thus overestimating its quantification. The findings of the present study are reserved only for patients with STEMI after fibrinolytic therapy, thus limiting the external validity of the findings.

## CONCLUSIONS

In this study, involving a small number of patients with STEMI, morphological characterization through intravascular ultrasound in grayscale and tissue US with iMAP™ technology, showed that there is a predominance of positive arterial remodeling and necrotic component in the composition of the culprit plaque, which supports the pathophysiology of atherosclerotic disease. The presence of plaque rupture, however, was prevalent in only 40% of cases. Future studies using new invasive imaging technologies with higher spatial resolution are needed to attain a better comprehension of the pathophysiology and better treatment promotion for patients with acute myocardial infarction with ST-segment elevation.

## CONFLICTS OF INTEREST

The authors declare no conflicts of interest.

## FUNDING SOURCES

The study had partial funding (donations of catheters) by Boston Scientific.

## REFERENCES

1. Fuster V, Moreno PR, Fayad ZA, Corti R, Badimon JJ. Atherothrombosis and high-risk plaque: part I: evolving concepts. *J Am Coll Cardiol*. 2005;46(6):937-54.
2. Otsuka F, Joner M, Prati F, Virmani R, Narula J. Clinical classification of plaque morphology in coronary disease. *Nat Rev Cardiol*. 2014;11(7):379-89.
3. Narula J, Nakano M, Virmani R, Kolodgie FD, Petersen R, Newcomb R, et al. Histopathologic characteristics of atherosclerotic coronary disease and implications of the findings for the invasive and noninvasive detection of vulnerable plaques. *J Am Coll Cardiol*. 2013;61(10):1041-51.
4. Hu S, Yonetsu T, Jia H, Karanasos A, Aguirre AD, Tian J, et al. Residual thrombus pattern in patients with ST-segment elevation myocardial infarction caused by plaque erosion versus plaque rupture after successful fibrinolysis: an optical coherence tomography study. *J Am Coll Cardiol*. 2014;63(13):1336-8.
5. Hu S, Jia H, Vergallo R, Abtahian F, Tian J, Soeda T, et al. Plaque erosion: in vivo diagnosis and treatment guided by optical coherence tomography. *JACC Cardiovasc Interv*. 2014;7(6):e63-4.
6. Matsuo Y, Takumi T, Mathew V, Chung WY, Barsness GW, Rihal CS, et al. Plaque characteristics and arterial remodeling in coronary and peripheral arterial systems. *Atherosclerosis*. 2012;223(2):365-71.
7. Pu J, Mintz GS, Biro S, Lee JB, Sum ST, Madden SP, et al. Insights into echo-attenuated plaques, echolucent plaques, and plaques with spotty calcification: novel findings from comparisons among intravascular ultrasound, near-infrared spectroscopy, and pathological histology in 2,294 human coronary artery segments. *J Am Coll Cardiol*. 2014;63(21):2220-33.
8. Kataoka Y, Wolski K, Uno K, Puri R, Tuzcu EM, Nissen SE, et al. Spotty calcification as a marker of accelerated progression of coronary atherosclerosis: insights from serial intravascular ultrasound. *J Am Coll Cardiol*. 2012;59(18):1592-7.
9. Trusinskis K, Juhnveica D, Strenge K, Erglis A. iMap intravascular ultrasound evaluation of culprit and non-culprit lesions in patients with ST-elevation myocardial infarction. *Cardiovasc Revasc Medicine*. 2013;14(2):71-5.
10. Souza CFd, Alves CMR, Carvalho AC, Bonfim AV, Silva EOdA, P. Junior EC, et al. Estudo iWONDER (Imaging Whole vessel coronary tree with intravascular ultrasound and iMap™ in patients with acute myocardial infarction): racional e desenho do estudo. *Rev Bras Cardiol Invasiva*. 2012;20(2):199-203.
11. Mintz GS, Nissen SE, Anderson WD, Bailey SR, Erbel R, Fitzgerald PJ, et al. American College of Cardiology Clinical Expert Consensus Document on Standards for Acquisition, Measurement and Reporting of Intravascular Ultrasound Studies (IVUS). A report of the American College of Cardiology Task Force on Clinical Expert Consensus Documents. *J Am Coll Cardiol*. 2001;37(5):1478-92.
12. Mintz GS, Garcia-Garcia HM, Nicholls SJ, Weissman NJ, Bruining N, Crowe T, et al. Clinical expert consensus document on standards for acquisition, measurement and reporting of intravascular ultrasound regression/progression studies. *Euro Intervention*. 2011;6(9):1123-30.
13. Xie Y, Mintz GS, Yang J, Doi H, Iniguez A, Dangas GD, et al. Clinical outcome of nonculprit plaque ruptures in patients with acute coronary syndrome in the PROSPECT study. *JACC Cardiovasc Imaging*. 2014;7(4):397-405.
14. Lee JB, Mintz GS, Lissauskas JB, Biro SG, Pu J, Sum ST, et al. Histopathologic validation of the intravascular ultrasound diagnosis of calcified coronary artery nodules. *Am J Cardiol*. 2011;108(11):1547-51.
15. Sathyanarayana S, Carlier S, Li W, Thomas L. Characterisation of atherosclerotic plaque by spectral similarity of radiofrequency intravascular ultrasound signals. *Euro Intervention*. 2009;5(1):133-9.
16. Falk E, Nakano M, Bentzon JF, Finn AV, Virmani R. Update on acute coronary syndromes: the pathologists' view. *Eur Heart J*. 2013;34(10):719-28.
17. Narula J, Garg P, Achenbach S, Motoyama S, Virmani R, Strauss HW. Arithmetic of vulnerable plaques for noninvasive imaging. *Nat Clin Pract Cardiovasc Med*. 2008;5 Suppl 2:S2-10.
18. Kolodgie FD, Burke AP, Farb A, Gold HK, Yuan J, Narula J, et al. The thin-cap fibroatheroma: a type of vulnerable plaque: the major precursor lesion to acute coronary syndromes. *Curr Opin Cardiol*. 2001;16(5):285-92.
19. Glagov S, Weisenberg E, Zarins CK, Stankunavicius R, Koletlis GJ. Compensatory enlargement of human atherosclerotic coronary arteries. *N Engl J Med*. 1987;316(22):1371-5.
20. Cascon-Perez JD, de la Torre-Hernandez JM, Ruiz-Abellon MC, Martinez-Pascual M, Marmol-Lozano R, Lopez-Candel J, et al. Characteristics of culprit atheromatous plaques obtained in vivo by intravascular ultrasound radiofrequency analysis: results from the CULPLAC study. *Am Heart J*. 2013;165(3):400-7.
21. Hong YJ, Jeong MH, Choi YH, Song JA, Ahmed K, Lee KH, et al. Positive remodeling is associated with vulnerable coronary plaque components regardless of clinical presentation: virtual histology-intravascular ultrasound analysis. *Int J Cardiol*. 2013;167(3):871-6.

22. Mehran R, Dangas G, Mintz GS, Lansky AJ, Pichard AD, Satler LF, et al. Atherosclerotic plaque burden and CK-MB enzyme elevation after coronary interventions: intravascular ultrasound study of 2256 patients. *Circulation*. 2000;101(6):604-10.
23. Watanabe T, Nanto S, Uematsu M, Ohara T, Morozumi T, Kotani J, et al. Prediction of no-reflow phenomenon after successful percutaneous coronary intervention in patients with acute myocardial infarction: intravascular ultrasound findings. *Circ J*. 2003;67(8):667-71.
24. Gyongyosi M, Wexberg P, Kiss K, Yang P, Sperker W, Sochor H, et al. Adaptive remodeling of the infarct-related artery is associated with recurrent ischemic events after thrombolysis in acute myocardial infarction. *Coron Artery Dis*. 2001;12(3):167-72.
25. Gyongyosi M, Yang P, Hassan A, Domanovits H, Laggner A, Weidinger F, et al. Intravascular ultrasound predictors of major adverse cardiac events in patients with unstable angina. *Clin Cardiol*. 2000;23(7):507-15.
26. Endo A, Hirayama H, Yoshida O, Arakawa T, Akima T, Yamada T, et al. Arterial remodeling influences the development of intimal hyperplasia after stent implantation. *J Am Coll Cardiol*. 2001;37(1):70-5.
27. Mintz GS, Tinana A, Hong MK, Lee CW, Kim JJ, Fearnot NE, et al. Impact of preinterventional arterial remodeling on neointimal hyperplasia after implantation of (non-polymer-encapsulated) paclitaxel-coated stents: a serial volumetric intravascular ultrasound analysis from the ASian Paclitaxel-Eluting Stent Clinical Trial (ASPECT). *Circulation*. 2003;108(11):1295-8.
28. Matsuo K, Ueda Y, Tsujimoto M, Hao H, Nishio M, Hirata A, et al. Ruptured plaque and large plaque burden are risks of distal embolisation during percutaneous coronary intervention: evaluation by angioscopy and virtual histology intravascular ultrasound imaging. *EuroIntervention*. 2013;9(2):235-42.
29. Calvert PA, Obaid DR, O'Sullivan M, Shapiro LM, McNab D, Densem CG, et al. Association between IVUS findings and adverse outcomes in patients with coronary artery disease: the VIVA (VH-IVUS in Vulnerable Atherosclerosis) Study. *JACC Cardiovasc Imaging*. 2011;4(8):894-901.
30. Stone GW, Maehara A, Lansky AJ, de Bruyne B, Cristea E, Mintz GS, et al. A prospective natural-history study of coronary atherosclerosis. *N Engl J Med*. 2011;364(3):226-35.
31. Marso SP, Mercado N, Maehara A, Weisz G, Mintz GS, McPherson J, et al. Plaque composition and clinical outcomes in acute coronary syndrome patients with metabolic syndrome or diabetes. *JACC Cardiovasc Imaging*. 2012;5(3 Suppl):S42-52.
32. Shimamura K, Ino Y, Kubo T, Nishiguchi T, Tanimoto T, Ozaki Y, et al. Difference of ruptured plaque morphology between asymptomatic coronary artery disease and non-ST elevation acute coronary syndrome patients: An optical coherence tomography study. *Atherosclerosis*. 2014;235(2):532-7.
33. Karanasos A, Ligthart JM, Witberg KT, Regar E. Calcified nodules: an underrated mechanism of coronary thrombosis? *JACC Cardiovasc Imaging*. 2012;5(10):1071-2.
34. Missel E, Mintz GS, Carlier SG, Sano K, Qian J, Kaple RK, et al. Necrotic core and its ratio to dense calcium are predictors of high-risk non-ST-elevation acute coronary syndrome. *Am J Cardiol*. 2008;101(5):573-8.
35. Takaoka N, Tsujita K, Kaikita K, Hokimoto S, Mizobe M, Nagano M, et al. Comprehensive analysis of intravascular ultrasound and angiographic morphology of culprit lesions between ST-segment elevation myocardial infarction and non-ST-segment elevation acute coronary syndrome. *Int J Cardiol*. 2014;171(3):423-30.